ADVANCES IN ATMOSPHERIC SCIENCES, VOL. 22, NO. 2, 2005, 159–171

Climate Change Signal Analysis for Northeast Asian Surface Temperature

Jeong-Hyeong LEE*[1], Byungsoo KIM[2], Keon-Tae SOHN[3], Won-Tae KOWN[4], and Seung-Ki MIN[4,5]

[1] *Division of Management Information Science, Dong-A University, Busan* 604-714

[2] *Department of Data Science, Inje University, Kimhae* 621-749

[3] *Department of Statistics, Pusan National University, Busan* 609-735

[4] *Climate Research Laboratory, Meteorological Research Institute, Korean Meteorological Administration, Seoul* 156-720

[5] *Meteorological Institute of the University of Bonn, Germany*

(Received 4 June 2004; revised 27 December 2004)

ABSTRACT

Climate change detection, attribution, and prediction were studied for the surface temperature in the Northeast Asian region using NCEP/NCAR reanalysis data and three coupled-model simulations from ECHAM4/OPYC3, HadCM3, and CCCma GCMs (Canadian Centre for Climate Modeling and Analysis general circulation model). The Bayesian fingerprint approach was used to perform the detection and attribution test for the anthropogenic climate change signal associated with changes in anthropogenic carbon dioxide (CO_2) and sulfate aerosol (SO_4^{2-}) concentrations for the Northeast Asian temperature. It was shown that there was a weak anthropogenic climate change signal in the Northeast Asian temperature change. The relative contribution of CO_2 and SO_4^{2-} effects to total temperature change in Northeast Asia was quantified from ECHAM4/OPYC3 and CCCma GCM simulations using analysis of variance. For the observed temperature change for the period of 1959–1998, the CO_2 effect contributed 10%–21% of the total variance and the direct cooling effect of SO_4^{2-} played a less important role (0%–7%) than the CO_2 effect. The prediction of surface temperature change was estimated from the second CO_2+SO_4^{2-} scenario run of ECHAM4/OPYC3 which has the least error in the simulation of the present-day temperature field near the Korean Peninsula. The result shows that the area-mean surface temperature near the Korean Peninsula will increase by about 1.1° by the 2040s relative to the 1990s.

Key words: climate change, detection, attribution, prediction, Northeast Asia

1. Introduction

The response of the global climate to external forcing mechanisms is inherently complex. Previous studies which attributed global-mean surface temperature increases over the last hundred years to anthropogenic forcings (e.g., Mitchell et al., 1995; Santer et al., 1996) relied on a few integrations of complex coupled atmosphere-ocean general circulation models (AOGCMs) and considered only a limited number of forcings. In reality, over the last hundred years, the Earth's energy balance has been altered by many natural and anthropogenic forcings (Shine and Forster, 1999). Although some forcings, such as changes in carbon dioxide (CO_2), can be reasonably well quantified, the magnitude and spatial pattern of some other possible forcings are poorly known, such as the indirect effect of sulphate aerosol (SO_4^{2-}) on clouds. There are also large uncertainties in the various feedback mechanisms and in the internal variability of the climate system. Due to the complex nature of the various feedbacks operating in the climate system, the simulation of the global surface temperature response with the AOGCMs is both computationally demanding and uncertain.

The most recent improvement in the climate signal detection problem is the inclusion of several possible sources of climate forcings. It has become apparent that when anthropogenic climate forcings are considered, one must include the forcings of greenhouse gases

*E-mail: jeonglee@donga.ac.kr

and sulfate aerosols (North and Stevens, 1998; Levine and Berliner, 1999; Berliner et al., 2000; Lee et al., 2001).

Since understanding and quantifying climatic changes at the regional scale is one of the most important and uncertain issues within the climate change debate, the need to provide regional climate change information has increased for both impact assessment studies and policymaking (Mearns et al., 2001). A regional climate is determined by interactions between large, regional and local scales, but the available tools have directed research toward understanding the climate system as a whole. In the Northeast Asian region, many climate models show that the increase of the atmospheric CO_2 should induce a long-term and spatially coherent warming and the increase of the atmospheric SO_4^{2-} should induce a long-term and spatially coherent cooling, though the warming and cooling might be relatively weak in some regions (Dai et al., 2001; Gao et al., 2001; Guo et al., 2001; Zeng et al., 2001).

To date, projections of regional climate changes for the twenty first century have been based on AOGCM simulations of the climate system response to changes in anthropogenic forcings (Kattenberg et al., 1996; Cubasch et al., 2001). The AOGCM information can then be enhanced with the use of "regionalization" techniques to obtain finer regional detail (Giorgi and Mearns, 1991; Giorgi et al., 2001).

An important step towards the understanding of regional climate changes and their impacts is the assessment of the characteristics of natural climate variability and the AOGCM performance in reproducing it. Climate variability can, in fact, mask anthropogenically forced signals, so that a characterization of the natural variability is necessary to evaluate the intensity of the forced change signal. In addition, the variability is often more important than the average climate in determining impacts on human and natural systems. Thus an assessment of the performance of models in simulating the observed variability can improve the interpretation of climate change simulations for impact applications.

In this study, we applied a detection technique known as Bayesian fingerprints and showed that decadal changes in the patterns of surface temperature in Northeast Asia can be explained partly by anthropogenic factors. Furthermore, we show that for regionally averaged surface temperature, internal noise in the AOGCM is small enough that a signal emerges from the data even on interannual timescales. Finally, although anthropogenic forcings have had a significant impact on global mean surface temperature, it is shown that their influence on the pattern of local deviations about this mean is hardly detectable, so its signal is weak.

The study is organized as follows. We start with descriptions of the AOGCM data and the observational datasets used in this study in section 2, followed by an explanation of the detection method and its application results for Northeast Asian temperature using the Bayesian fingerprint approach in section 3. In section 4, the relative contribution of the CO_2 and SO_4^{2-} effects to total temperature change is examined using analysis of variance. The prediction of surface temperature change in Northeast Asia by the 2040s is estimated from an AOGCM simulation in section 5. Finally, conclusions are given in section 6.

2. Data and regions

We used the surface temperature of three AOGCM simulations: ECHAM4/OPYC3, HadCM3, and the Canadian Centre for Climate Modeling and Analysis general circulation model (CCCma GCM). Model details and arrangements for our experiments are described by Roeckner et al. (1992), DKRZ (1992) and Oberhuber (1993a, b) for ECHAM4/OPYC3, Gordon et al. (2000) and Pope et al. (2000) for HadCM3, and Lohmann et al. (1997, 1999a, b) for CCCma GCM. Description of the experimental design and the results by the three AOGCMs (ECHAM4/OPYC3, HadCM3, and CCCma GCM) are summarized in Table 1 and plotted in Fig. 1. All climate change simulations are based on IS92a greenhouse (G) or greenhouse plus sulfate aerosols (GS) scenarios. In the tables, CO_2+SO_4^{2-} forcing (1), CO_2+SO_4^{2-} forcing (2) and CO_2+SO_4^{2-} forcing (3) are the repeated results from the same scenario but different initial conditions. So we considered them as different scenario runs. We also used the National Centers for Environmental Prediction (NCEP) and the National Center for Atmospheric Research (NCAR) Collaborative Reanalyses (hereafter, NNR) for observed predictors. This is a 51-yr (1948–1998) record of global analyses of atmospheric fields produced using a frozen global data assimilation system (Kistler et al., 2001).

Since the statistical model applicability is highly dependent on the quality of the predictors, the control climatologies of the coupled models were first compared with the NNR. All model fields were spatially interpolated to the $5^\circ \times 5^\circ$ grid of NNR because the data structures of the above GCM outputs are the $5^\circ \times 5^\circ$ grid. Comparisons were carried out for yearly means over the 40 model years for the domain of 30°–60°N and 120°–150°E which covers most of Northeast Asia in order to track most of the circulation patterns that affect the Korean peninsula.

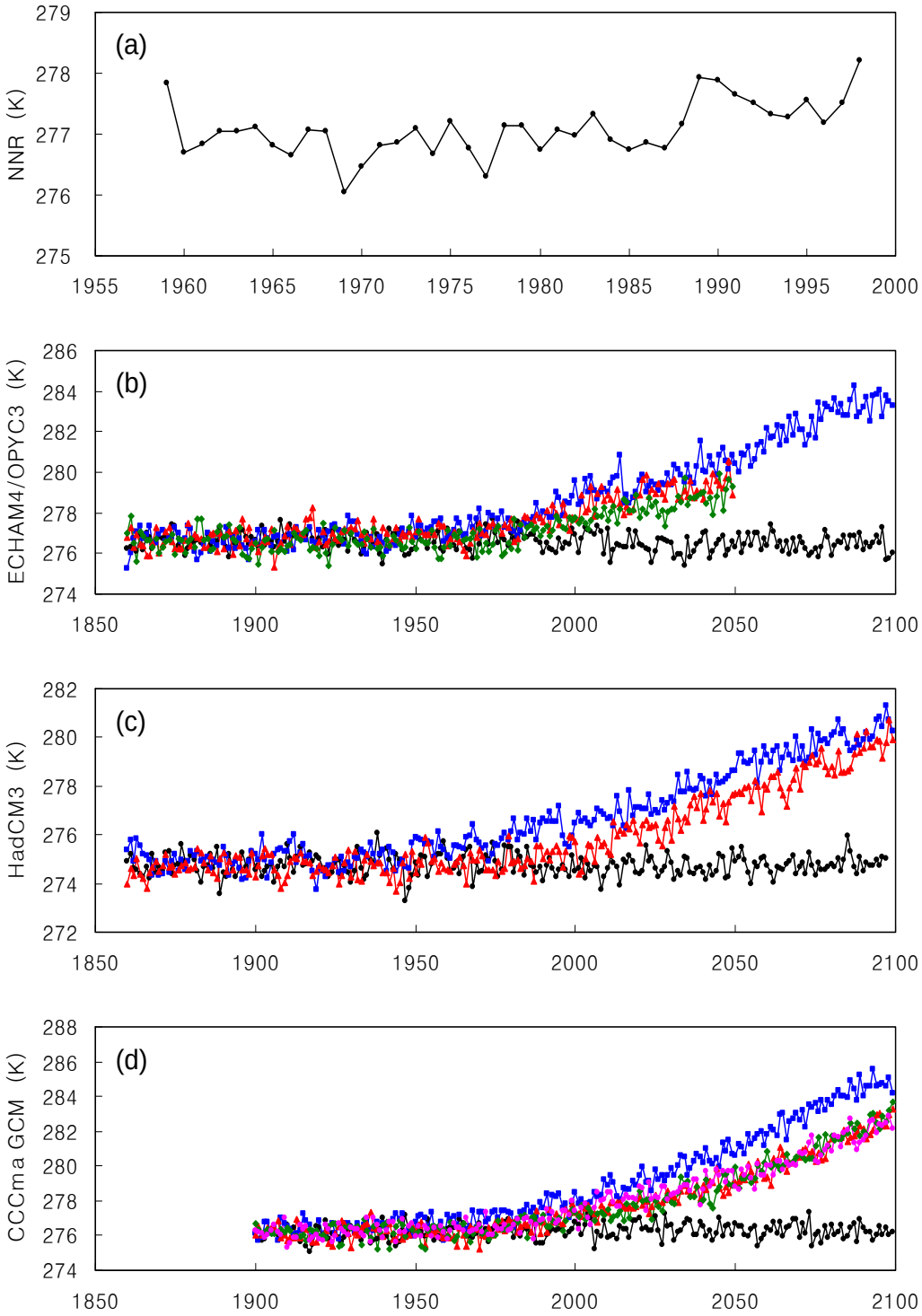

Fig. 1 Regional average of yearly mean surface air temperature: (a) NNR, (b) ECHAM4/OPYC3 [●: control run, ■: CO_2 forcing, ▲: CO_2+SO_4^{2-} forcing (1), ◆: CO_2+SO_4^{2-} forcing (2)], (c) HadCM3 (●: control run, ■: CO_2 forcing, ▲: CO_2+SO_4^{2-}), and (d) CCCma GCM [●: control run, ■: CO_2 forcing, ▲: CO_2+SO_4^{2-} forcing (1), ◆: CO_2+SO_4^{2-} forcing (2), ●: CO_2+SO_4^{2-} forcing (3)].

Table 1. List of AOGCM simulations used in this study.

GCM	Experiment	Forcing scenario
ECHAM4/OPYC3	control run	constant CO_2
	CO_2, forcing	historic CO_2 1860–1989, IS92a 1990–2099
	CO_2+SO_4^{2-} forcing(1)	historic CO_2 1860–1989, IS92a 1990–2049
		historic SO_4^{2-} 1860–1989, IS92a 1990–2049
	CO_2+SO_4^{2-} forcing(2)	historic CO_2 1860–1989, IS92a 1990–2049
		historic SO_4^{2-} 1860–1989, IS92a 1990–2049
HadCM3	control run	constant CO_2
	CO_2 forcing	historic CO_2 1900–1989, IS92a 1990–2100
	CO_2+SO_4^{2-} forcing	historic CO_2 1900–1989, IS92a 1990–2100
		historic SO_4^{2-} 1900–1989, IS92a 1990–2100
CCCma GCM	control run	constant CO_2
	CO_2 forcing	historic CO_2 1900–1989, IS92a 1990–2100
	CO_2+SO_4^{2-} forcing(1)	historic CO_2 1900–1989, IS92a 1990–2100
		historic SO_4^{2-} 1900–1989, IS92a 1990–2100
	CO_2+SO_4^{2-} forcing(2)	historic CO_2 1900–1989, IS92a 1990–2100
		historic SO_4^{2-} 1900–1989, IS92a 1990–2100
	CO_2+SO_4^{2-} forcing(3)	historic CO_2 1900–1989, IS92a 1990–2100
		historic SO_4^{2-} 1900–1989, IS92a 1990–2100

3. Detection and attribution of anthropogenic effects

3.1 *Bayesian fingerprint approach*

Berliner et al. (2000) proposed a Bayesian fingerprint approach for assessing anthropogenic impacts on climate. The modeling process formalizes the relation

$$\text{Observations} = a \times \boldsymbol{g} + \text{noise}\,, \tag{1}$$

where a is an unknown parameter, $\boldsymbol{g}$ is a spatially varying scenario run fingerprint, and "noise" is modeled to account for both errors in the data and natural climate variability. Our analysis will be for the unknown amplitude a introduced in Eq. (1). The formal mechanism for Bayes' Theorem yields the posterior distribution:

$$\pi(a|\text{data}) \propto f(\text{data}|a)\pi(a)\,, \tag{2}$$

where $\pi(a)$ is the prior distribution and $f(\text{data}|a)$ is the conditional distribution of the data given a, often known as the likelihood function. An intuitive interpretation of Bayes' Theorem is that once the data have been observed, the prior distribution is reweighted by the likelihood function to produce the posterior one. General reviews can be found in Berger (1985), Epstein (1985), and Bernardo and Smith (1994).

Define vectors of observations $\boldsymbol{Y}_1, \ldots, \boldsymbol{Y}_m$, where $\boldsymbol{Y}_t$ represents the observed annual temperatures in year $t = 1, \ldots, m$. Let $\boldsymbol{Y} = (\boldsymbol{Y}'_1, \ldots, \boldsymbol{Y}'_m)'$ be the collection of these vectors. Our data model includes a formal adjustment for errors present in the observations. We assume that these errors all have mean zero, are independent from year to year, and have normal distributions. This is summarized for each year as

$$\boldsymbol{Y}_t|a, \boldsymbol{g}, \boldsymbol{\Sigma}_\text{s} \sim N(\boldsymbol{g}a, \boldsymbol{\Sigma}_\text{s}) \tag{3}$$

where n is the number of grid points, $\boldsymbol{\Sigma}_\text{s}$ is an $n \times n$ spatial covariance matrix, $\boldsymbol{g}$ is an n-vector denoting the fingerprint, and $N(\cdot, \cdot)$ represents the probability density function for a normal distribution; the first argument is the mean and the second is the variance. Note that, as in the fingerprint work of Hasselmann (1997) and the references therein, we assume that the fingerprint pattern is constant over time. Alternatively, we can represent the model for all observations as

$$\boldsymbol{Y}|a, \boldsymbol{g}, \boldsymbol{D}, \boldsymbol{\Sigma} \sim N(\boldsymbol{G}a, \boldsymbol{D} + \boldsymbol{\Sigma})\,, \tag{4}$$

where $\boldsymbol{D}$ is a block diagonal matrix with an $n \times n$ covariance matrix of true run, $\boldsymbol{G}$ is an $m \cdot n$-vector of $\boldsymbol{g}$. The matrix $\boldsymbol{\Sigma}$ is equal to $\boldsymbol{\Sigma}_\text{c} \otimes \boldsymbol{\Sigma}_\text{s}$, where $\boldsymbol{\Sigma}_\text{c}$ is an $m \times m$ correlation matrix for an autoregressive process of order one and $\otimes$ denotes the Cartesian product. We focus on the modeling and inference for the amplitude a here.

Both Bayesian and traditional fingerprint approaches to statistical inference benefit from application of the so-called sufficiency principle (Berger, 1985, 126–127; Epstein, 1985, 23–25). The idea is to construct functions of the data which summarize all the statistical information contained in the data regarding the unknown parameter. It turns out that for the model Eq. (4), a sufficient statistic for a is the generalized least squares estimator (GLS), denoted by $\hat{a}(\boldsymbol{Y})$.

This estimator is given by

$$\hat{a}(\boldsymbol{Y}) = (\boldsymbol{G}'\boldsymbol{V}^{-1}\boldsymbol{G})^{-1}\boldsymbol{G}'\boldsymbol{V}^{-1}\boldsymbol{Y} \tag{5}$$

where $\boldsymbol{V} = \boldsymbol{D} + \boldsymbol{\Sigma}, \hat{a}(\boldsymbol{Y})$ is the best linear unbiased estimator. A further result from statistics (Graybill, 1976) implies that

$$\hat{a}(\boldsymbol{Y})|a \sim N(a, \sigma^2) \tag{6}$$

where

$$\sigma^2 = (\boldsymbol{G}'\boldsymbol{V}^{-1}\boldsymbol{G})^{-1} . \tag{7}$$

In summary, we base our Bayesian inferences about a only on Eq. (6) and our prior on a. The issues of climate change motivate construction of the prior $\pi(a)$ as a mixture of two main components as follows: with probability p, a has a normal distribution with mean 0 and variance τ^2, and with probability $1 - p, a$ has a normal distribution with mean μ_A and variance τ_A^2. Symbolically, we write

$$\pi(a) = pN(0, \tau^2) + (1 - p)N(\mu_A, \tau_A^2) , \tag{8}$$

The first component of Eq. (8) is to model information about a under the qualitative statement that anthropogenic CO_2 or CO_2+SO_4^{2-} forcings do not impact global temperatures, at least not in a fashion reflected by the fingerprint $\boldsymbol{g}$. The selection of zero as the prior mean of a in this component of the prior seems quite natural. The variance τ^2 is interpreted as the variability, arising naturally, anticipated in fitting a by projecting temperature fields onto the selected fingerprint $\boldsymbol{g}$. The probability p is then a quantification of the degree of belief in the hypothesis of no anthropogenic impacts. The second component of the prior represents an implied distribution on a assuming significant anthropogenic effects representable as changes in temperature patterns along the fingerprint $\boldsymbol{g}$. The quantity μ_A is the hypothesized shift in a, which in turn translates into shifts in temperature anomalies $\boldsymbol{g}a$. The variance τ_A^2 reflects anticipated variability in a under CO_2 or CO_2+SO_4^{2-} forcings. This parameter reflects, in part, natural climate variability, though there is no requirement that $\tau_A^2 = \tau^2$.

The variation represented by τ^2 would be best estimated through replications of the climate system under AOGCM control run output. Prior parameters, μ_A and τ_A^2 under CO_2 or CO_2+SO_4^{2-} forcings were computed from CO_2 or CO_2+SO_4^{2-} forced outputs.

For a prior of the mixture form Eq. (8), the posterior distribution is also a mixture (e.g., Berger, 1985, 127–128, 206). We have

$$\begin{aligned}\pi(a|\hat{a}) =& p(\hat{a})N[\mu(a|\hat{a}), \tau^2(a|\hat{a})] \\ &+ [(1 - p(\hat{a})N][\mu_A(a|\hat{a}), \tau_A^2(a|\hat{a})] ,\end{aligned} \tag{9}$$

where

$$\begin{aligned}\mu_A(a|\hat{a}) &= \frac{\tau_A^2}{\tau_A^2 + \sigma^2}\hat{a} + \frac{\tau_A^2}{\tau_A^2 + \sigma^2}\mu_A , \\ \tau_A^2(a|\hat{a}) &= \frac{\tau_A^2\tau^2}{\tau_A^2 + \sigma^2} ,\end{aligned} \tag{10}$$

and

$$\begin{aligned}p(\hat{a}) = &\left\{1 + \left(\frac{1-p}{p}\right)\sqrt{\frac{\tau^2 + \sigma^2}{\tau_A^2 + \sigma^2}}\right. \\ &\left.\times \exp\left[-\frac{1}{2}\left(\frac{(\hat{a} - \mu_A)^2}{\tau_A^2 + \sigma^2} - \frac{\hat{a}^2}{\tau^2 + \sigma^2}\right)\right]\right\}^{-1} .\end{aligned} \tag{11}$$

This distribution is a mixture of the two posteriors corresponding to each of the two components of the prior Eq. (8). The mixing weight $p(\hat{a})$ is a function of the observed data. It is important to note that $p(\hat{a})$ is not necessarily interpretable as the posterior probability that the no-change prior distribution is correct. Rather, it is a weight associated with the corresponding posterior distribution. Indeed, depending on the data, either one or both of the components of the posterior distribution Eq. (9) may be very different from their corresponding priors.

We next formalize the specialized inspections of the posterior distribution intended to serve as Bayesian procedures for detection and attribution. We define "no significant climate change" to be the event that $a \in D$, where D is some neighborhood of zero. Similarly, we define another set A, a neighborhood of the mean μ_A, to represent an attribution set which reflects the physics of CO_2 or CO_2+SO_4^{2-} impacts on climate.

With these definitions, we can use the Bayesian model for inferences regarding detection and attribution. Detection is defined as when the posterior probability that a departs significantly from 0 is large; namely, if $Pr(a \in D|\hat{a})$ is small. Attribution occurs when both the posterior probability $Pr(a \in A|\hat{a})$ s large and $1 - p(\hat{a})$ is large. The two requirements in the statement of attribution need not be redundant. To learn about the Bayesian fingerprint approach in detail, see Berliner et al. (2000).

3.2 *Detection and attribution results*

We present posterior inferences using four subsets of three AOGCM datasets corresponding to the time periods: (a) 1959–1998, (b) 1969–1998, (c) 1979–1998, and (d) 1989–1998. The year 1959 was chosen as the initial time point since the baseline from which the NNR data was computed begins in 1959. These four time periods are suggested since climate change trends are anticipated to be increasingly more visible during the latter part of the twentieth century. It should be

noted that we should use different priors for a depending on the time period analyzed.

Tables 2 to 4 present the generalized least square estimates $\hat{a}$ of the amplitude of fingerprint a defined in Eq. (5) and the associated standard deviations σ computed from Eq. (7) for each of the four time periods considered. Note that σ increases as the time windows get shorter. Tables 2 to 4 also present the means and standard deviations in Eq. (10) and Eq. (11) for the two components of the posterior distribution in Eq. (9) and the posterior weight $p(\hat{a})$ in Eq. (11) assuming the prior weight $p = 0.5$. Figure 2 displays the prior and posterior distributions of a for $p = 0.5$. The plot also shows the likelihood functions derived from Eq. (6). Note that the posterior distributions are unimodal for time periods (a) to (d). The unimodality is a consequence of the posterior mixture probability $p(\hat{a})$ which is essentially zero or one. Thus, the posterior distribution in these time periods is solely the component of the posterior distribution under the no change scenario. These results generally suggest that the data most resemble the component of the posterior distributions corresponding to no change; this behavior seems overwhelming for the most recent time periods. The probability $p(\hat{a})$ is the "no change" component of the posterior model, as a function of the prior probability p. The posterior probability $p(\hat{a})$ is nearly near one for all time periods. In fact, for $p = 0.5, p(\hat{a})$ is about 1, providing more weight for the "no change" component of the posterior distribution. If the posterior probabilities $p(\hat{a})$ lie well below 0.5 for most of the range of p, then this places substantial weight on the "anthropogenic forcing" component of the posterior distribution.

Table 2. List of values of parameters in the Bayesian fingerprint approach using NCEP/NCAR reanalysis and ECHAM4/OPYC3 CO_2 and CO_2+SO_4^{2-} (1)–(2) runs for the time periods of 1959–1998, 1969–1998, 1979–1998, and 1989–1998: $\hat{a}$ is likelihood in Eq. (6), σ is the standard deviation of likelihood function in Eq. (7), τ is the standard deviation of the first component of the prior mixture in Eq. (8), $\mu_{\hat{a})}$ and τ_A are the mean and standard deviation of the second component of the prior mixture in Eq. (8), $\mu(a \mid \hat{a})$ and $\tau(a \mid \hat{a})[\mu_A(a \mid \hat{a})$ and $\tau_A(a \mid \hat{a})]$ are the mean and standard deviation of the first [second] component of the posterior mixture in Eq. (9), and $p(\hat{a})$ is the posterior weight in Eq. (12). All values are in the case of the prior weight $p = 0.5$.

Scenario	Period	$\hat{a}$	σ	τ	μ_A	τ_A	$\mu(a \mid \hat{a})$	$\tau(a \mid \hat{a})$	$\mu_A(a \mid \hat{a})$	$\tau_A(a \mid \hat{a})$	$p(\hat{a})$
CO_2	1959–1998	–0.0411	0.0231	0.0120	0.9299	0.2303	–0.0087	0.0106	–0.0314	0.0230	0.9999
	1969–1998	0.0098	0.0265	0.0178	0.9170	0.2588	0.0030	0.0148	0.0193	0.0264	0.9997
	1979–1998	–0.0054	0.0326	0.0233	0.9247	0.2939	–0.0018	0.0190	0.0059	0.0324	0.9990
	1989–1998	0.0004	0.0454	0.0393	0.9292	0.3121	0.0003	0.0297	0.0200	0.0450	0.9974
CO_2+SO_4^{2-}(1)	1959–1998	0.0577	0.0566	0.0345	1.2900	0.1204	0.0156	0.0295	0.2814	0.0512	0.9999
	1969–1998	0.0428	0.0651	0.0667	1.2917	0.2191	0.0219	0.0466	0.1442	0.0624	0.9999
	1979–1998	0.0059	0.0803	0.0891	1.2843	0.2940	0.0032	0.0596	0.0947	0.0775	0.9999
	1989–1998	0.0017	0.1131	0.1454	1.3110	0.3486	0.0010	0.0892	0.1264	0.1076	0.9991
CO_2+SO_4^{2-}(2)	1959–1998	0.0132	0.0691	0.0420	1.5560	0.1402	0.0035	0.0359	0.3150	0.0620	0.9999
	1969–1998	–0.0078	0.0802	0.0697	1.5317	0.1494	–0.0033	0.0526	0.3367	0.0707	0.9999
	1979–1998	0.0224	0.0987	0.0846	1.5360	0.2243	0.0095	0.0642	0.2688	0.0904	0.9999
	1989–1998	–0.0005	0.1389	0.1435	1.5223	0.3623	–0.0002	0.0998	0.1947	0.1297	0.9997

Table 3. Same as Table 2 except for HadCM3 CO_2 and CO_2+SO_4^{2-} runs.

Scenario	Period	$\hat{a}$	σ	τ	μ_A	τ_A	$\mu(a \mid \hat{a})$	$\tau(a \mid \hat{a})$	$\mu_A(a \mid \hat{a})$	$\tau_A(a \mid \hat{a})$	$p(\hat{a})$
CO_2	1959–1998	–0.0512	0.0279	0.0312	0.9620	0.2178	–0.0284	0.0208	–0.0347	0.0277	0.9999
	1969–1998	–0.0149	0.0324	0.0344	0.9594	0.2509	–0.0079	0.0236	0.0010	0.0322	0.9998
	1979–1998	–0.0195	0.0383	0.0393	0.9680	0.2794	–0.0100	0.0274	–0.0013	0.0379	0.9995
	1989–1998	–0.0034	0.0535	0.0471	0.9626	0.3067	–0.0015	0.0353	0.0250	0.0527	0.9981
CO_2+SO_4^{2-}	1959–1998	–0.0558	0.0299	0.0264	0.9839	0.2153	–0.0244	0.0197	–0.0361	0.0296	0.9999
	1969–1998	–0.0964	0.0350	0.0305	0.9762	0.2563	–0.0416	0.0230	–0.0767	0.0347	0.9997
	1979–1998	–0.0234	0.0407	0.0335	0.9779	0.2690	–0.0094	0.0258	–0.0009	0.0403	0.9997
	1989–1998	–0.0012	0.0562	0.0419	0.9727	0.3004	–0.0004	0.0336	0.0316	0.0552	0.9985

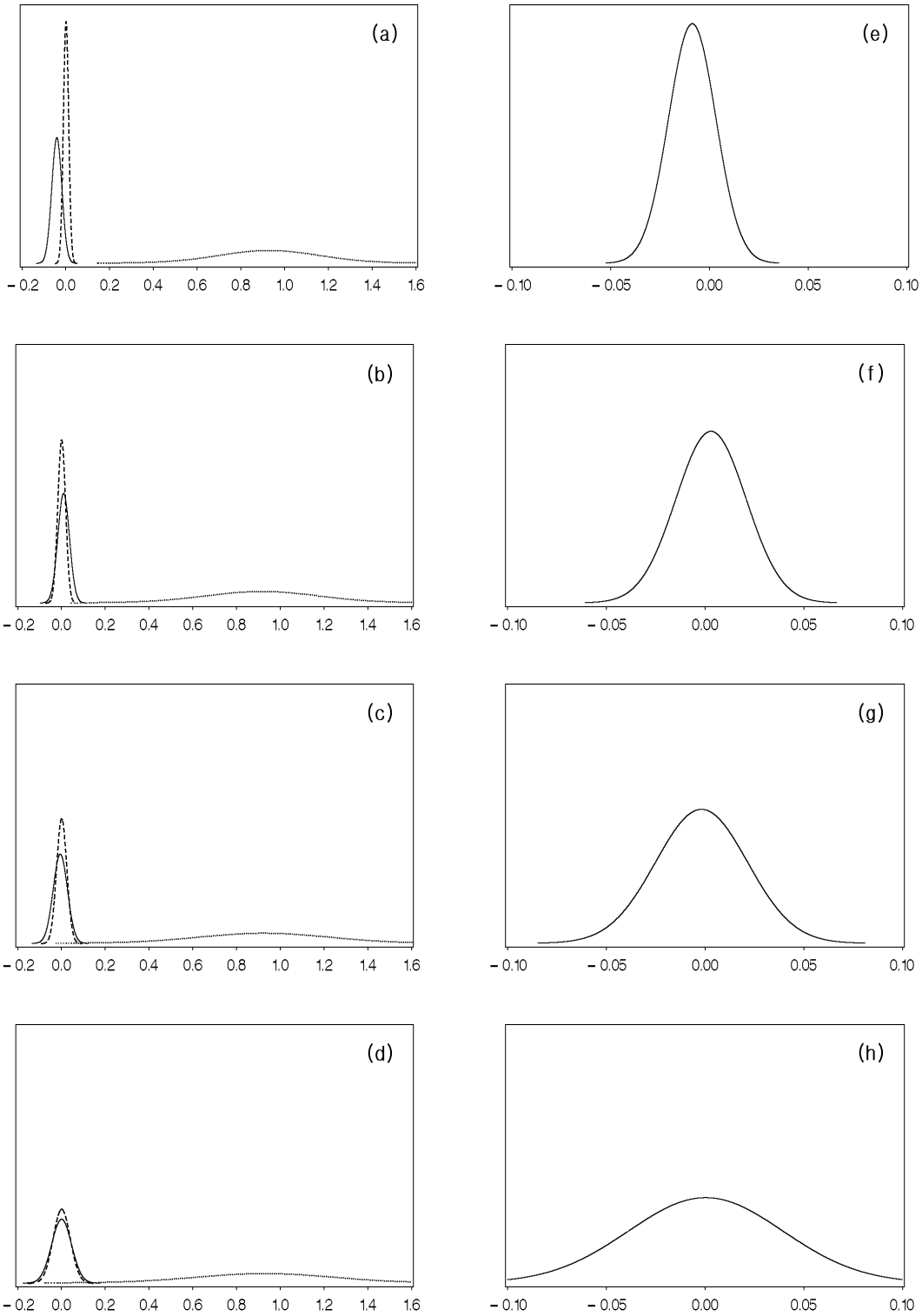

Fig. 2. Likelihood function, prior distribution, and posterior distribution of a using ECHAM4/OPYC3 fingerprint of Northeast Asia for the four time periods of 1959–1998, 1969–1998, 1979–1998, and 1989–1998: (a)–(d) are the likelihood (solid line) and prior distribution components [anthropogenic CO_2 forcing (dotted line); no anthropogenic impacts (dashed line)], respectively, and (e)–(h) are the posterior mixture distribution, respectively.

Table 4. Same as Table 2 except for CCCma GCM CO_2 and CO_2+SO_4^{2-} (1)–(3) runs.

Scenario	Period	$\hat{a}$	σ	τ	μ_A	τ_A	$\mu(a \mid \hat{a})$	$\tau(a \mid \hat{a})$	$\mu_A(a \mid \hat{a})$	$\tau_A(a \mid \hat{a})$	$p(\hat{a})$
CO_2	1959–1998	–0.0209	0.0187	0.0084	0.9303	0.2983	–0.0035	0.0076	–0.0172	0.0187	0.9992
	1969–1998	–0.0307	0.0219	0.0175	0.9244	0.3370	–0.0120	0.0137	–0.0267	0.0218	0.9972
	1979–1998	0.0108	0.0268	0.0236	0.9353	0.3645	0.0047	0.0177	0.0158	0.0267	0.9958
	1989–1998	0.0016	0.0385	0.0402	0.9355	0.4123	0.0008	0.0278	0.0097	0.0383	0.9895
CO_2+SO_4^{2-}(1)	1959–1998	–0.0148	0.0220	0.0101	0.9317	0.2972	–0.0025	0.0092	–0.0096	0.0220	0.9993
	1969–1998	–0.0435	0.0259	0.0231	0.9234	0.3404	–0.0193	0.0172	–0.0380	0.0258	0.9959
	1979–1998	0.0224	0.0319	0.0312	0.9382	0.3781	0.0109	0.0223	0.0289	0.0318	0.9927
	1989–1998	0.0030	0.0470	0.0504	0.9395	0.4223	0.0016	0.0344	0.0145	0.0467	0.9858
CO_2+SO_4^{2-}(2)	1959–1998	–0.0226	0.0224	0.0114	0.9216	0.2897	–0.0046	0.0101	–0.0170	0.0223	0.9993
	1969–1998	–0.0473	0.0262	0.0250	0.9127	0.3307	–0.0225	0.0181	–0.0413	0.0261	0.9961
	1979–1998	0.0210	0.0322	0.0338	0.9331	0.3732	0.0110	0.0233	0.0278	0.0321	0.9929
	1989–1998	0.0033	0.0474	0.0530	0.9357	0.4270	0.0017	0.0353	0.0147	0.0471	0.9844
CO_2+SO_4^{2-}(3)	1959–1998	–0.0159	0.0218	0.0104	0.9414	0.2610	–0.0029	0.0094	–0.0092	0.0217	0.9998
	1969–1998	–0.0448	0.0255	0.0247	0.9348	0.2984	–0.0216	0.0177	–0.0377	0.0255	0.9987
	1979–1998	0.0213	0.0316	0.0339	0.9517	0.3282	0.0114	0.0231	0.0299	0.0315	0.9970
	1989–1998	0.0035	0.0463	0.0535	0.9490	0.3790	0.0020	0.0350	0.0175	0.0460	0.9914

Table 5. Significance probabilities for detection and attribution test results from ECHAM4/OPYC3 scenario runs. "Detection" has very small values; "attribution" may be suggested by moderate or large values.

Scenario		Time period			
		1959–1998	1969–1998	1979–1998	1989–1998
CO_2	Detection	0.8503	0.8139	0.7047	0.4976
	Attribution	0.1232	0.7782	0.6984	0.4976
CO_2+SO_4^{2-}(1)	Detection	0.4449	0.2991	0.2620	0.1771
	Attribution	0.2091	0.3021	0.2621	0.1771
CO_2+SO_4^{2-}(2)	Detection	0.4201	0.2952	0.2416	0.1587
	Attribution	0.4085	0.2948	0.2395	0.1587

Table 6. Same as Table 5 except for HadCM3.

Scenario		Time period			
		1959–1998	1969–1998	1979–1998	1989–1998
CO_2	Detection	0.3323	0.5765	0.5047	0.4275
	Attribution	0.4270	0.5818	0.5074	0.4273
CO_2+SO_4^{2-}	Detection	0.3987	0.1074	0.5304	0.4479
	Attribution	0.2782	0.0646	0.4972	0.4478

Tables 5 to 7 show the posterior probabilities of the detection and attribution regions, $Pr(a \in D|\hat{a})$ and $Pr(a \in A \mid \hat{a})$, for the three AOGCMs (ECHAM4/OPYC3, HadCM3, CCCma), as functions of p, for the four time periods. We selected $D = [0 - 0.02, 0 + 0.02]$ and $A = [\mu_A - 0.02, \mu_A + 0.02]$ using a similar way to Berliner et al. (2000). The latter proposed that when the posterior probabilities of D lie within a range of zero to 0.5, a climate change signal of anthropogenic forcing is detected, and when the posterior probabilities of A lie within a range of 0.3–1.0 the detected climate change signal in the observation is attributed to the anthropogenic forcing.

Table 5 shows the ECHAM4/OPYC3 results. The detection result for the CO_2 simulation shows large probabilities for the detection region for all periods, suggesting no evidence of a detected signal under CO_2 forcing. The detection results for CO_2+SO_4^{2-} simulations represent moderate probabilities for the detection region for time period (a), implying no evidence

Table 7. Same as Table 5 except for CCCma GCM.

Scenario		Time period			
		1959–1998	1969–1998	1979–1998	1989–1998
CO_2	Detection	0.9823	0.7084	0.7228	0.5256
	Attribution	0.6288	0.5343	0.7120	0.5256
CO_2+SO_4^{2-}(1)	Detection	0.9628	0.5017	0.5727	0.4363
	Attribution	0.7991	0.3979	0.5688	0.4369
CO_2+SO_4^{2-}(2)	Detection	0.9256	0.4340	0.5560	0.4257
	Attribution	0.5794	0.3881	0.5650	0.4260
CO_2+SO_4^{2-}(3)	Detection	0.9569	0.4527	0.5664	0.4305
	Attribution	0.7711	0.4206	0.5698	0.4305

of a detected signal, but they represent small probabilities for the detection region for time periods (b), (c), and (d), indicating little evidence of a detected signal under CO_2+SO_4^{2-}(1) and CO_2+SO_4^{2-}(2) forcings. That is, there is some suggestion of a detected change based on time periods (b), (c), and (d) in that $Pr(a \in D|\hat{a}) < 0.5$ for $p = 0.5$. The attribution results of the ECHAM4/OPYC3 CO_2 simulation shows that there is strong evidence for attribution to periods (b), (c), and (d) of the CO_2 forcing since the corresponding posterior probability $Pr(a \in A|\hat{a})$ is of the order of 0.5 to 0.8. However, there is little evidence for attribution to the CO_2+SO_4^{2-}(1) and CO_2+SO_4^{2-}(2) forcings represented in our ECHAM4/OPYC3-based fingerprint.

The result from HadCM3 (Table 6) shows moderate or large probabilities for the detection region for all periods, implying no evidence of a detected signal under CO_2 and CO_2+SO_4^{2-} forcings except in (b) for CO_2+ SO_4^{2-} and that there is strong evidence for attribution to the CO_2 forcing while there is little evidence for attribution to the CO_2+SO_4^{2-} forcing except for period (b). The result from the CCCma GCM (Table 7) shows large probabilities for the detection region for all periods, implying no evidence of a detected signal under CO_2 and all three CO_2+SO_4^{2-} forcings, and that there is strong evidence for attribution to periods (b), (c), and (d) of the CO_2 and all CO_2+SO_4^{2-} forcings.

4. Quantification of anthropogenic effects

We used analysis of variance for a quantification measure of components for changes in surface air temperature. Our regression model was as follows:

$$Y = \beta_0 + \beta_1 X_1 + \beta_2 X_2 + \varepsilon$$

where Y ={NCEP/NCAR reanalysis–control run}, X_1 ={Scenario run(CO_2)–control run}, X_2 ={scenario run (CO_2+SO_4^{2-})–scenario run(CO_2)}. In the regression model, the analysis of variance approach is based on the partitioning of sums of squares associated with the response variable Y. The least squares fitting process, thus, provides a partition of the total variability into a component that is attributed to the fitted line (SSR) and a component that is due to departures from that line (SSE). That is,

$$S_{\rm t} = S_{\rm r} + S_{\rm e} \ ,$$

where $S_{\rm t}$ stands for the total sum of squares, $S_{\rm r}$ stands for the regression sum of squares, and $S_{\rm e}$ stands for the error sum of squares. In multiple regression, we can obtain a variety of decompositions of $S_{\rm r}$ in the extra sum of squares. An extra sum of squares measures the marginal reduction in the error sum of squares when one or several independent variables are added to the regression model given that other independent variables are already in the model. An extra sum of squares involves the difference between the two corresponding regression sums of squares (Von Storch and Zwiers, 1999). If X_1 is the extra variable, we have:

$$S_{\rm r}(X_1|X_2) = S_{\rm r}(X_1, X_2) - S_{\rm r}(X_2) \ .$$

We present relative contributions of CO_2 and SO_4^{2-} to total surface temperature change using four subsets of two AOGCM datasets and the four time periods: (a) 1959–1998, (b) 1969–1998, (c) 1979–1998, and (d) 1989–1998. For each of the four time periods, Tables 8–12 present two type decompositions of the regression sum of squares into extra sum of squares and their ratio for CO_2+SO_4^{2-} simulations with ECHAM4/OPYC3 and CCCma GCM. The ratio stands for the proportion of total variation associated with the independent variable, X_1 or X_2, and $S_{\rm s}$ stands for the sum of squares.

The result of the ECHAM4/OPYC3 CO_2+SO_4^{2-}(1) in Table 8 shows that surface temperature variability by the CO_2 effect is about 7% to 18% when SO_4^{2-} is the extra variable and it is about 7% to 23% when CO_2 is the extra variable. On the other hand, surface temperature variability by the SO_4^{2-} effect is about 1%

Table 8. Contribution ratio of CO_2 (X_1) and SO_4^{2-} (X_2) to the total temperature change in Northeast Asia inferred from ECHAM4/OPYC3 CO_2 and CO_2+SO_4^{2-}(1) runs.

Time period	Source	$S_s(X_1)$	$S_s(X_z \mid X_1)$	S_e
1959–1998	S_s	300.46	98.39	1692.58
	Ratio	0.1437	0.0470	0.8093
1969–1998	S_s	308.22	85.68	1312.63
	Ratio	0.1806	0.0502	0.7692
1979–1998	S_s	175.97	32.12	949.61
	Ratio	0.1520	0.0277	0.8203
1989–1998	S_s	35.78	6.26	460.68
	Ratio	0.0712	0.0125	0.9164

Table 9. Same as Table 8 except for ECHAM4/OPYC3 CO_2 and CO_2+SO_4^{2-}(2) runs.

Time period	Source	$S_s(X_1)$	$S_s(X_z \mid X_1)$	S_e
1959–1998	S_s	300.46	153.05	1637.92
	Ratio	0.1437	0.0732	0.7832
1969–1998	S_s	308.22	101.44	1296.86
	Ratio	0.1806	0.0594	0.7599
1979–1998	S_s	175.97	58.17	923.56
	Ratio	0.1520	0.0502	0.7978
1989–1998	S_s	35.78	17.53	449.42
	Ratio	0.0712	0.0349	0.8940

Table 10. Same as Table 8 except for CCCma GCM CO_2 and CO_2+SO_4^{2-}(1) runs.

Time period	Source	$S_s(X_1)$	$S_s(X_z \mid X_1)$	S_e
1959–1998	S_s	1005.60	25.64	7871.36
	Ratio	0.1130	0.0029	0.8842
1969–1998	S_s	1267.58	145.29	5526.02
	Ratio	0.1827	0.0209	0.7964
1979–1998	S_s	928.47	419.20	3506.55
	Ratio	0.1913	0.0864	0.7224
1989–1998	S_s	891.38	265.83	1339.89
	Ratio	0.3570	0.1065	0.5366

Table 11. Same as Table 8 except for CCCma GCM CO_2 and CO_2+SO_4^{2-} (2) runs.

Time period	Source	$S_s(X_1)$	$S_s(X_z \mid X_1)$	S_e
1959–1998	S_s	1005.60	43.54	7853.45
	Ratio	0.1130	0.0049	0.8822
1969–1998	S_s	1267.58	84.47	5586.85
	Ratio	0.1827	0.0122	0.8051
1979–1998	S_s	928.47	305.05	3620.70
	Ratio	0.1913	0.0628	0.7459
1989–1998	S_s	891.38	354.07	1251.64
	Ratio	0.3570	0.1418	0.5012

Table 12. Same as Table 8 except for CCCma GCM CO_2 and CO_2+SO_4^{2-}(3) runs.

Time period	Source	$S_s(X_1)$	$S_s(X_z \mid X_1)$	S_e
1959–1998	S_s	1005.60	197.24	7699.75
	Ratio	0.1130	0.0222	0.8649
1969–1998	S_s	1267.58	217.28	5454.04
	Ratio	0.1827	0.0313	0.7860
1979–1998	S_s	92.847	310.29	3615.46
	Ratio	0.1913	0.0639	0.7448
1989–1998	S_s	891.38	336.95	1268.76
	Ratio	0.3570	0.1349	0.5081

Table 13. RMSE of 40-yr (1959–1998) mean surface temperature near the Korean Peninsula.

AOGCM	Scenario	RMSE
ECHAM4/OPYC3	CO_2	1.9953
	CO_2+SO_4^{2-}(1)	1.7195
	CO_2+SO_4^{2-}(2)	1.5736
CCCma GCM	CO_2	2.6111
	CO_2+SO_4^{2-}(1)	2.6658
	CO_2+SO_4^{2-}(2)	2.6710
	CO_2+$SO_4$2−(3)	2.5966

to 5% when SO_4^{2-} is the extra variable and it is about 0% to less than 1% when CO_2 is the extra variable.

The result of ECHAM4/OPYC3 CO_2+SO_4^{2-}(2) in Table 9 shows similar results.

Over all, the results of the ECHAM4/OPYC3 scenario runs provide evidence that the CO_2 effect of ECHAM4/OPYC3 is about 14% to 23% from 1959 to 1998 and the SO_4^{2-} effect of ECHAM4/OPYC3 is about 0% to 7% from 1959 to 1998. These results indicate that the effect of anthropogenic forcings of CO_2 and SO_4^{2-} explains a part of the surface temperature increase in Northeast Asia. The results of three CO_2+SO_4^{2-} simulations with CCCma GCM (from Tables 10 to 12) show that the CO_2 effect is about 9% to 12% from 1959 to 1998 and the SO_4^{2-} effect is about 0% to 2% from 1959 to 1998. It is suggested that for the decadal timescale, climate change signals can be detected on a regional scale although with a weak amplitude.

5. Projection of surface temperature near the korean peninsula

Using seven scenario runs from ECHAM4/OPYC3 and CCCma GCM, we examined which scenario run is most similar to NNR over the 1959 to 1998 periods

with a 2.5° × 2.5° grid spacing on a domain near the Korean Peninsula from 32.5°N to 45°N and 122.5°E to 132.5°E. The main statistical tool used for this comparison is the root mean square error (RMSE) between the AOGCMs scenario runs and NNR surface temperature. The RMSE (σ_e) is defined as

$$\sigma_e = \left[\frac{1}{L}\sum_{k=1}^{L}(y_k - o_k)^2\right]^{1/2},$$

where $y_k = CO_2 - NNR$ or $y_k = (CO_2 + SO_4^{2-}) - NNR$, $o_k = NNR$ and L is the total number of grid points in the domain.

Table 13 summarizes the RMSE between the AOGCMs scenario runs and NNR surface temperature. The comparison result shows that the $CO_2 + SO_4^{2-}$(2) scenario run of ECHAM4/OPYC3 is most similar to NNR.

Table 14 shows the decadal surface temperature changes from the 2000s to the 2040s under the CO_2+SO_4^{2-}(2) scenario of ECHAM4/OPYC3 over the Korean peninsula. It can be seen that the warming starts from about 0.2°C in the 2000s to 1.1°C in the 2040s. The surface temperature changes have a highly significant warming effect for all periods.

Table 14. Prediction of temperature change near the Korean Peninsula from ECHAM4/OPYC3 CO_2+SO_4^{2-}(2) runs.

Period	2000–2009	2010–2019	2020–2029	2030-2039	2040-2049
Variation of	0.2253	0.4560	0.5103	0.9722	1.0884
temperature (°C)	(0.0341)	(0.0484)	(0.0295)	(0.0512)	(0.0613)
t-statistic	6.61	9.42	17.24	18.95	17.75
p-value	< 0.0001	< 0.0001	< 0.0001	< 0.0001	< 0.0001

( ): standard error.

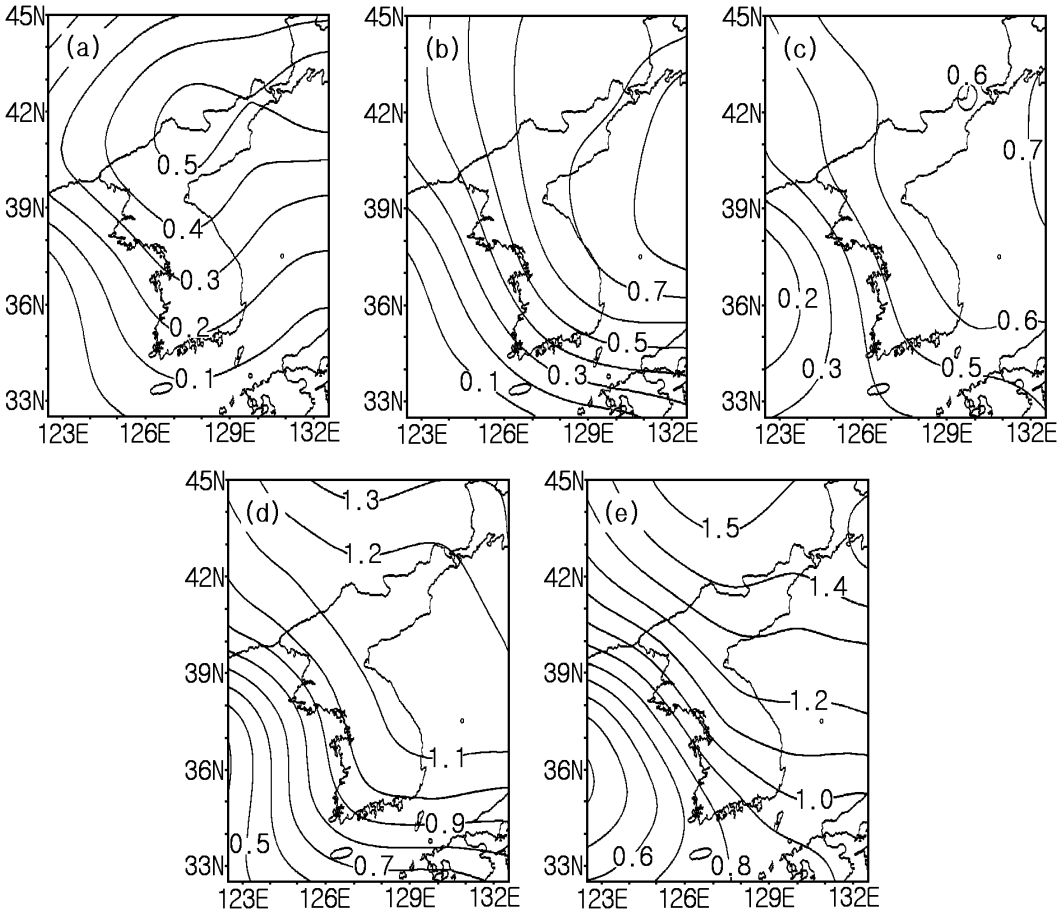

Fig. 3. Horizontal patterns of surface temperature change in the 2000s to the 2040s estimated from ECHAM4/OPYC3 CO_2+SO_4^{2-}(2): (a) 2000s, (b) 2010s, (c) 2020s, (d) 2030s, and (e) 2040s.

Figure 3 shows the horizontal pattern of mean surface temperature change for the 2000s to the 2040s of the CO_2+SO_4^{2-}(2) scenario of ECHAM4/OPYC3. It shows that the temperature increase becomes larger with time and that the increase in the northern part is a little larger than in the southern part.

6. Concluding remarks

We performed a climate change detection and attribution test of the anthropogenic signal associated with changes in CO_2 and SO_4^{2-} concentrations for Northeast Asia from the ECHAM4/OPYC3, HadCM3, and CCCma GCM simulations using a Bayesian fingerprint approach. We found a weak evidence of a detected signal under CO_2 and CO_2+SO_4^{2-} forcings and a stronger evidence for attribution to the CO_2 and CO_2+SO_4^{2-} forcings represented in our fingerprints.

In addition, we performed a quantification of components of climate change and prediction of variation of surface temperature to 2049 based on scenario runs of ECHAM4/OPYC3, HadCM3, and CCCma GCMs in Northeast Asia. In the scenario run of ECHAM4/OPYC3, the CO_2 effect of climate change is 14% to 21% in 1959 to 1998 and the SO_4^{2-} effect of climate change is 0 to 7% from 1959 to 1998. In the scenario run of the CCCma GCM, the CO_2 effect of climate change is 10 to 12% from 1959 to 1998 and the SO_4^{2-} effect of climate change is 0 to 3% from 1959 to 1998.

The model validation was done in the context of RMSE for the present day temperature field, and the CO_2 +SO_4^{2-}(2) scenario run of ECHAM4/OPYC3 turned out to have the best performance of temperature near the Korean Peninsula. Using the best scenario run, the temperature prediction was estimated to 2049; it is projected that a warming of about 1.1°C will appear in the 2040s near the Korean Peninsula. However, it should be noted that there is much uncertainty in this prediction because it came from a single realization of a single coupled model. A multimodel ensemble method from a number of simulations from both AOGCMs and Regional Climate Model (RCMs) can be a promising way to reduce the uncertainty in the prediction of regional climate change.

Acknowledgments. This research was performed for the Greenhouse Gas Research Center, one of the Critical Technology Programs funded by the Ministry of Science and Technology of Korea.

REFERENCES

Aiguo Dai, G. A. Meehl, W. M. Washington, and T. M. L. Wigley, 2001: Climate change in the 21st Century over the Asia-Pacific region simulated by the NCAR CSM and PCM. *Adv. Atmos. Sci.*, **18**, 639–658.

Berger, J. O., 1985: *Statistical Decision Theory and Bayesian Analysis*. 2nd ed., Springer-Verlag, 617pp.

Berliner, L. M., R. A. Levine, and D. J. Shea, 2000: Bayesian climate change assessment. *J. Climate*, **13**, 3805–3820.

Bernardo, J. M., and A. F. M. Smith, 1994: *Bayesian Theory*. Wiley & Sons, 586pp.

Cubasch, U., and Coauthors, 2001: *Climate Change 2001: The Scientific Basis. Contribution of Working Group I to the Third Assessment Report of the Intergovernmental Panel on Climate Change IPCC*, Cambridge University Press, Cambridge, UK, 525–582.

Deutsches KlimaRechenzentrum (DKRZ), 1992: The ECHAM3 general circulation model. *DKRZ Technical Report*, **6**, ISSN 0940–9327, Modellbetreuungsgruppe Hamburg, 184pp.

Epstein, E. S., 1985: *Statistical Inference and Prediction in Climatology: A Bayesian Approach*. Amer. Meteor. Soc., 199pp.

Gao, X., Z. Zhao, Y. Ding, R. Huang, and F. Giorgi, 2001; Climate change due to greenhouse effects in China as simulated by a regional climate model. *Adv. Atmos. Sci.*, **18**, 1224–1230.

Giorgi, F., B. Hewitson, J. Christensen, M. Hulme, H. von Storch, P. Whetton, R. Jones, and L. Fu C. Mearns, 2001: *Climate Change 2001: The Scientific Basis. Contribution of Working Group I to the Third Assessment Report of the Intergovernmental Panel on Climate Change IPCC*, Cambridge University Press, Cambridge, UK, 583–638.

Gordon, C., C. Cooper, C. A. Senior, H. Banks, J. M. Gregory, T. C. Johns, J. F. B. Mitchell, and R. A. Wood, 2000: The simulation of SST, sea ice extents and ocean heat transports in a version of the Hadley Centre coupled model without flux adjustments. *Climate Dyn.*, **16**, 147–168.

Graybill, F. A., 1976: *Theory and Application of the Linear Model*. Duxbury Press, 704pp.

Guo, Y., Y. Yu, X. Liu, and X. Zhang, 2001; Simulation of climate change induced by CO_2 increasing for East Asia with IAP/LASG GOALS model. *Adv. Atmos. Sci.*, **18**, 53–66.

Hasselmann, K., 1997: Multi-pattern fingerprint method for detection and attribution of climate change. *Climate Dyn.*, **13**, 601–611.

Kattenberg, A, and Coauthors, 1996: *Climate Change 1995: The Science of Climate Change. Contribution of Working Group I to the Second Assessment Report of the Intergovernmental Panel on Climate Change IPCC*, Cambridge University Press, Cambridge, UK, 285–327.

Kistler, R., E., and Coauthors, 2001: The NCEP/NCAR 50-year reanalysis: Monthly means CD-ROM and documentation. *Bull. Amer. Meteor. Soc.*, **82**, 247–267.

Lee, J. H., K. T. Sohn, and B. Kim, 2001: Detection of anthropogenic climate change signal in East Asian region. *Journal of the Korean Data Analysis Society*, **3**,

217–225. (in Korean)

Levine, R. A., and L. M. Berliner, 1999: Statistical principles for climate change studies. *J. Climate*, **12**, 565–574.

Lohmann, U., and J. Feichter, 1997: Impact of sulfate aerosols on albedo and lifetime of clouds. *J. Geophys. Res.*, **102**, 13685–13700.

Lohmann, U., K. von Salzen, N. McFarlane, H. G. Leighton, and J. Feichter, 1999a: Tropospheric sulphur cycle in the Canadian general circulation model. *J. Geophys. Res.*, **104**, 26833–26858.

Lohmann, U., N. McFarlane, L. Levkov, K. Abdella, and F. Albers, 1999b: Comparing different cloud schemes of a single column model by using mesoscale forcing and nudging technique. *J. Climate*, **12**, 438–461.

Mearns, L. O., M. Hulme, T. R. Carter, R. Leemans, M. Lal, and P. Whetton, 2001: *Climate Change 2001: The Scientific Basis. Contribution of Working Group I to the Third Assessment Report of the Intergovernmental Panel on Climate Change IPCC*, Cambridge University Press, Cambridge, UK, 739–768.

Mitchell, J. F. B., T. C. Johns, and J. M. Gregory, and S. F. B. Tett, 1995: Climate response to increasing levels of greenhouse gases and sulfate aerosols. *Nature*, **376**, 501–504.

North, G, R., and M. J, Stevens, 1998: Detecting climate signals in the surface temperature record. *J. Climate*, **11**, 563–577.

Oberhuber, J. M., 1993a: Simulation of the Atlantic circulation with a coupled sea-ice-mixed layer-isopycnical general circulation model. Part I: Model description. *J. Phys. Oceanogr.*, **23**, 808–829.

Oberhuber, J. M., 1993b: Simulation of the Atlantic circulation with a coupled sea-ice-mixed layer-isopycnical general circulation model. Part II: Model experiment. *J. Phys. Oceanogr.*, **23**, 830–845.

Pope, V. D., M. L. Gallani, P. R. Rowntree, and R. A. Stratton, 2000: The impact of new physical parameterizations in the Hadley Centre climate model HadAM3. *Climate Dyn.*, **16**, 123–146.

Roeckner, E., and Coauthors, 1992: Simulation of the present-day climate with the ECHAM model: Impact of model physics and resolution. Max-Planck Institute for Meteorology, Report No.93, Hamburg, 171pp.

Santer, B. D., and Coauthors, 1996: A search for human influences on the thermal structure of the atmosphere. *Nature*, **382**, 616–619.

Shine, K. P., and P. M. de F. Forster, 1999: The effect of human activity on radiative forcing of climate change: A review of recent developments. *Global Planet Change*, **20**, 205–225.

von Storch, H., and F. W. Zwiers, 1999: *Statistical Analysis in Climate Research*. Cambridge University Press, 484pp.

Zeng Zhaomei, Yan Zhongwei, and Ye Duzheng, 2001; The regions with the most significant temperature trends during the last century. *Adv. Atmos. Sci.*, **18**, 481–496.